European Journal of Wood and Wood Products (2025) 83:61
https://doi.org/10.1007/s00107-025-02214-2

ORIGINAL ARTICLE

Focus on hydrochars produced from hydrothermal liquefaction of beech wood, soda lignin and black liquor

Maximilian Wörner[1] · **Ursel Hornung**[1] · **Selhan Karagöz**[1,2] · **Thomas Zevaco**[1] · **Nicolaus Dahmen**[1]

Received: 13 October 2024 / Accepted: 26 January 2025

Abstract

Previous studies on the hydrothermal liquefaction (HTL) of biomass have primarily focused on bio-oil production, overlooking the significant hydrochar by-product. In this work, the HTL of beech wood, soda lignin, and black liquor was performed at temperatures of 300 °C and 350 °C for 20 min. The effect of temperature and biomass type on hydrochar yields and properties was thoroughly investigated. The mass yields of the hydrochars varied between 25.92 wt% and 32.70 wt%. An increase in temperature from 300 °C to 350 °C led to a decrease in hydrochar mass yields. The carbon yield was found to be highest (51 wt%) at 300 °C using beech wood. The highest heating value, 30.97 MJ/kg, was obtained with hydrochar derived from soda lignin at 300 °C. Solid-state carbon NMR demonstrated that the hydrochars derived from black liquor contain condensed aromatic structures. Both the type of biomass and temperature significantly influenced the characteristics of the resulting hydrochar. This research demonstrates that hydrochar holds promise as a solid biofuel due to its advantageous energy content and carbon yield, highlighting its potential for sustainable energy applications.

1 Introduction

Fossil fuels are finite resources and significant contributors to greenhouse gas emissions, driving global warming and climate change. As fossil fuel reserves decline and environmental concerns intensify, the demand for renewable energy sources is rapidly increasing. Lignocellulosic biomass is an important renewable resource due to its abundance, cost-effectiveness, environmental benefits, versatility, and non-competition with food production (Ragauskas et al. 2006; Isikgor and Becer 2015; Soh and Eckelman 2016; Zhan et al. 2022). This biomass can be utilized through several conversion technologies to produce energy and biofuels. The HTL process uses high temperatures, typically ranging from 250 °C to 400 °C, along with pressure and water, to convert biomass into a renewable form of crude bio-oil (Tekin et al. 2014). This approach offers a way to handle different types of biomasses, including those with high moisture levels, without the need for pre-drying. By keeping water in its liquid state during processing, it facilitates the creation of ionic reaction conditions. The applied temperature is high enough to initiate pyrolytic reactions in the biomass, while the pressure maintains water in its liquid phase throughout the process (Elliott et al. 2015). While the utilization of sub/supercritical water environments offers broad applicability and numerous advantages mentioned above, certain challenges persist within this methodology that necessitate process refinement. A key challenge arises from the requirement for high pressures during processing, which calls for reactor and separator designs involving significant capital costs, especially for large-scale operations (Zanon Costa et al. 2020). The bio-oils produced through HTL of lignocellulosic biomass exhibit a significantly higher energy density compared to the original biomass (Toor et al. 2011). Most research on HTL of lignocellulosic biomass to date has concentrated on the yield and composition of bio-oil (Nan et al. 2016; Madsen et al. 2017; Alper et al. 2019; Dahdouh et al. 2023).

The solid by-product, hydrochar, is generated in significant quantities during the HTL of biomass, with yields typically ranging from 20 to 45 wt%, depending on the type of

✉ Ursel Hornung
ursel.hornung@kit.edu

✉ Selhan Karagöz
skaragoz@karabuk.edu.tr

[1] Institut für Katalyseforschung und Technologie (IKFT), Karlsruher Institut für Technologie (KIT), 76344 Eggenstein-Leopoldshafen, Germany

[2] Department of Chemistry, Karabük University, Karabük 78050, Turkey

biomass and the operational parameters (Elliott et al. 2015; De Caprariis et al. 2017; Aykaç et al. 2018; Tai et al. 2021). Despite this, most research on the HTL of lignocellulosic biomass has concentrated on the yield and composition of bio-oil, often overlooking hydrochars, which are a valuable byproduct with significant potential applications. Few studies focused on hydrochar yields and properties from the HTL of lignocellulosic biomasses (Hu et al. 2014; Jayathilake et al. 2021).

This manuscript aims to fill the existing gap by focusing on the yields and detailed properties of hydrochars produced from various biomasses, an area that has received limited attention in the literature. In the present study, hydrochar yields and characteristics from beech wood (BW) soda lignin (SL) and black liquor (BL) produced from the HTL process at 300 and 350 °C for 20 min were comparatively investigated. Notably, previous studies focusing on the HTL of lignin (Cao et al. 2020), beech wood (Haarlemmer et al. 2016), and black liquor (Harisankar and Vinu 2023) have highlighted their potential for bio-oil production and their distinct characteristics during the HTL process.

This study examines the influence of temperature and the type of feedstock on the yields and characteristics of hydrochars.

2 Methods

2.1 Biomass feedstock

Beech wood was supplied by Sappi Company (Stockstadt, Germany). Soda lignin was obtained from LignoPure GmbH (Hamburg, Germany). Black liquor was sourced from a pulp mill in Figueira da Foz, Portugal, operated by The Navigator Company. The selection of lignin, beech wood, and black liquor for the HTL experiments was based on their abundance and significant relevance to the wood and wood-related industries. The properties of biomasses used in this work are shown in Table 1. The density of BL was 1.0725 kg/L.

2.2 HTL experiments

HTL experiments for beech wood and soda lignin were conducted in a 2 L in-house constructed autoclave (1.4571/316Ti). The reactor had a maximum temperature of 500 °C and a maximum pressure of 50 MPa. In a typical run, 135 g of biomass (BW or SL) and 1.350 kg of deionized water were placed into the reactor. The reactor was heated to the specified temperatures of 300 °C and 350 °C and maintained at these levels for 20 min. For the 2 L reactor, the heating time to reach the desired temperature was 30–35 min for each run under continuous stirring. At the end of the reaction, the reactor was rapidly cooled to room temperature using a fan. Due to the limited quantity of black liquor samples available, HTL experiments for BL were conducted in stainless steel microreactors (1.4571/316Ti) with a volume of 25 mL. The filling levels were based on the water density at the specific temperatures and pressures. A pressure range of 200 to 250 bar was set as the target. In this study experiments were conducted at 300 °C and 350 °C, which lead to a filling level of 15 mL. In the case of micro-reactors, heating was conducted using a fluidized sand bath (SBL 2, Techne, Stone, UK). The heating time to reach the desired temperature was 10 min for each run. At the end of the reaction, the reactor was quenched to with a water bath. Once the HTL experiments were completed, vacuum filtration was employed to separate the liquid and solid residues. The solid residue, known as hydrochars, was dried in an oven at 105 °C for 24 h.

The hydrochar mass yield was determined using the following equation:

$$\text{Yield of hydrochars (wt\%)} = \frac{\text{mass of recovered solid products (g)}}{\text{mass of starting material (g)}} \times 100$$

The HTL experiments were repeated three times, and the reported results represent the mean of these replicates. The standard deviations for hydrochar yields in experiments conducted with micro-reactors were less than ±1 wt%, while for the 2 L reactor, they were less than ±2 wt%. Carbon yields of the hydrochars were calculated using the following equation:

Table 1 Elemental compositions (wt.%), atomic ratios, and higher heating values (HHV) of raw materials used

	Elemental Composition, wt%									
Raw materials	C	H	N	S	O[c]	Na	K	O/C[d]	H/C[d]	HHV, MJ kg^{-1}
Beech Wood (BW)[a]	44.14	6.25	0.14	-	49.47	-	-	0.84	1.70	15.01
Soda Lignin (SL)[a]	59.87	6.00	0.63	0.70	32.80	-	-	0.41	1.20	23.02
Dry Matter (BL)	34.00	3.40	<0.1	4.70	57.90	17.7	1.3	1.28	1.20	6.46
Extracted KL (BL)[b]	60.30	5.70	<0.1	2.60	31.40	0.4	<0.1	0.39	1.13	23.16

[a]dry basis, [b]extracted Kraft Lignin (Organic), [c] by difference, [d]atomic ratios

$$\text{Carbon Yields of hydrochars (wt\%)} = \frac{\text{mass of carbon} \in \text{solid products (g)}}{\text{mass of carbon} \in \text{starting materials (g)}} \times 100$$

As the aim of this study was to focus on hydrochars, the yields of neither gas nor biocrude or water-soluble products were determined.

2.3 Analytical methods

Single pulse 13 C MAS/CP-MAS NMR spectra of the hydrochars were obtained under standard conditions (1010 mbar, 20 °C) using a Jeol Spectrometer from the JNM-ECZR series, fitted with a 9.4 T Oxford Cryomagnet (resonance: 13 C @100.51621 MHz, 1 H @ 399.90513 MHz). The solid-state spectra were acquired using a JEOL Automas solid-state probe head. Further details regarding the 13 C NMR can be referenced in our previous publication (Wörner et al. 2024). The carbon (C), hydrogen (H), and sulfur (S) contents of the hydrochars were determined using an elemental analyzer (Vario EL Cube, Elementar Analysetechnik GmbH, Hanau, Germany) based on the combustion principle. Oxygen content was calculated by subtracting the sum of C, H, N, and S from 100. The higher heating values (HHV) were estimated using the Dulong equation, where C, H, O, N, and S correspond to the mass percentages of carbon, hydrogen, oxygen, nitrogen, and sulfur on a dry basis.

Dulong equation:

$$\text{HHV}\left(\frac{\text{MJ}}{\text{kg}}\right) = (0.338 \times \text{C}) + 1.428 \times \left(\text{H} - \frac{\text{O}}{8}\right) + (0.095 \times \text{S})$$

A thermogravmetric (TG) analyzer (Mettler Toledo DSC 822 at a heating rate of 10 °C /min) was used to determine ash content and volatile matter. N_2 (for determining volatile matter) and air (for determining ash content) were used as carrier gases at a flow rate of 50 mL/min. In a typical TG analysis, ~10 mg of sample was placed into a ceramic crucible and heated to 1000 °C from 25 °C. The volatile matter (VM) and ash (A) contents of the hydrochars were determined according to ASTM E1131.

The fixed carbon (FC) was determined from the following equation:

FC, wt% =100 - (VM, wt% +A, wt%).

The energy densification ratio (EDR) was determined using the formula below:

$$\text{EDR} = \frac{\text{Higher heating values of hydrochars}}{\text{Higher heating values of biomass}}$$

The energy yield (EY, %) of the hydrochars was estimated using the equation provided below:

$$\text{EY (\%)} = \text{Hydrochar mass yields (\%) x EDR}$$

The fuel ratio (FR) was calculated using the following equation.

$$\text{FR} = \text{FC}/\text{VM}$$

The surface topography of hydrochars was examined using an FEI Quanta FEG 650 Scanning Electron Microscope (SEM). The organic phase of the liquid product after HTL was extracted with ethyl acetate (EtOAc). Different compounds in the extracted organic phase were determined using a gas chromatograph (GC 6890 N Agilent, Santa Clara, CA, USA) equipped with a mass-selective (MS) detector (5973 MSD). Selected compounds in organic phase were quantified using a gas chromatograph (GC 7820 A) equipped with a flame ionization detector (FID). Pentadecane was employed as an internal standard (ISTD) for the quantification of compounds in the organic phases.

3 Results and discussion

3.1 Carbon and mass yields of hydrochars

Figure 1 illustrates the carbon yields of hydrochars obtained from BW, SL, and BL at temperatures of 300 and 350 °C for 20 min. Notably, hydrochars derived from BW exhibited the highest carbon yield. Carbon yields for BW, SL, and BL were 51 wt%, 41 wt%, and 35 wt% respectively, at 300 °C. As the temperature increased from 300 °C to 350 °C, the carbon yields decreased for BW and SL, while in the case of BL, the carbon yield slightly increased with temperature elevation. At 350 °C, the carbon yields for SL and BL were ~38 wt%, while BW had a carbon yield of ~45 wt%. The mass yields of hydrochars at 300 °C were similar for BW, SL, and BL, with slight variations (Table 2). At 350 °C, the mass yields decreased for all feedstocks. It is considered that a secondary decomposition of previously degraded species occurred, resulting in their conversion into gaseous products at 350 °C. Table S1 (provided in the Supplementary Material) presents the mass yields of hydrochars obtained in this study, along with the reported mass yields of hydrochars from the HTL of various biomass sources in the literature. The obtained hydrochar mass yields were found to be comparable to those reported in the literature (Zhong and Wei 2004; Cheng et al. 2010; De Caprariis et al. 2017; Tai et al. 2021; Harisankar and Vinu 2023; Rivas-Arrieta et al. 2024; Vadlamudi et al. 2024).

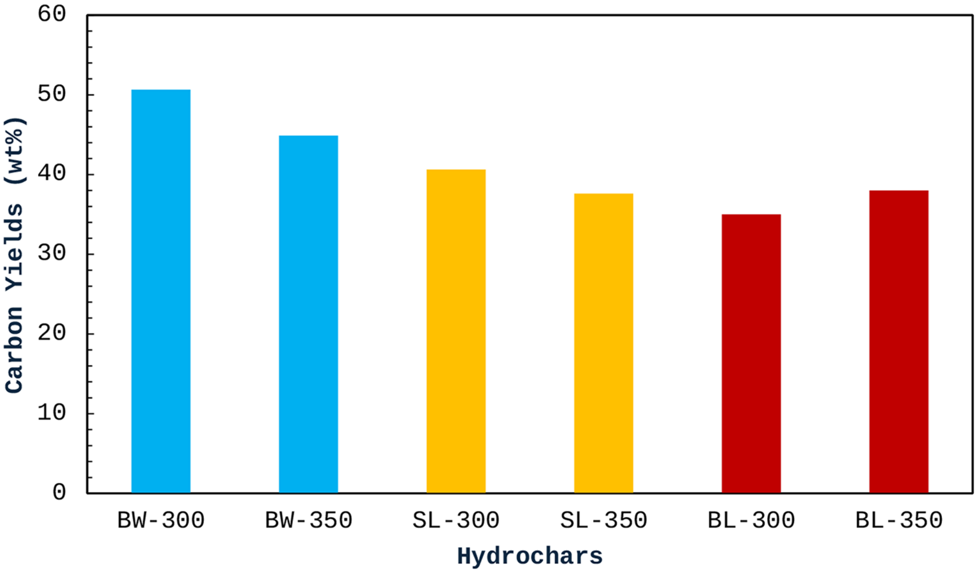

Fig. 1 Carbon yields of hydrochars produced from HTL of BW, SL, and BL at 300 and 350 °C

3.2 Properties of hydrochars

Table 2 shows the properties of hydrochars produced from the HTL of BW, SL and BL at 300 and 320 °C for 20 min. With increasing the temperature, the weight percentages of VM decreased and weight percentages of FC increased for all hydrochars. At 350 °C, the weight% values of FC were found to be 53.95 wt% for BW, 51.03 wt% for SL, and 52.24 wt% for BL, demonstrating consistent values across all feedstock types. It can be concluded that 350 °C is the optimum temperature to obtain hydrochars containing approximately 50 wt% of FC from any type of lignocellulose. The FR values of hydrochar produced at 300 °C varied between 0.78 and 0.97. As the temperature rose from 300 to 350 °C, the FR values of all hydrochars increased. This improvement in FR values can be attributed to the reduction in VM content and the simultaneous increase in FC content of hydrochars. The FR values of hydrochars obtained at 350 °C ranged from 1.11 to 1.39, and these values were comparable to those reported in the literature where the primary focus was obtaining hydrochar from lignocellulosic biomass via the hydrothermal carbonization (HTC) process. For example, the FR value (FR = 1.39) of hydrochar obtained from BL at 350 °C for 20 min. Exceeded those derived from Kraft lignin at 260 °C for 6 h (FR = 1.24) (Musa et al. 2022) and hydrochar from wheat straw at 240 °C for 1 h (FR = 0.55) (Ma et al. 2018), as reported in the literature.

The ash content of hydrochars from BL was higher than those obtained with BW and SL, which is due to the high inorganic content of BL. The ash contents of hydrochars obtained from BL were 18.90 wt% at 300 °C and 10.15 wt% at 350 °C. The decrease in ash content can be explained by the rising soluble inorganic content with increasing temperature.

Following HTL, hydrochars exhibited improved HHVs compared to their original biomasses. In terms of HHV of hydrochar, following the HTL, the order was SL > BW > BL. The heating values of hydrochars from SL were slightly higher than those corresponding to BW, which is an anticipated outcome. Additionally, an increase in the lignin ratio within wood leads to higher heating values (Demirbaş 2001; Vassilev et al. 2012). The heating value of BL is lower primarily due to the presence of inorganic salts as mentioned above. The accumulation of these salts during the pulping process leads to a reduction in the heating value of BL. It can be inferred that the heating values of hydrochars vary depending on the biomass sources from which they are derived. The heating values were higher at 350 °C than at 300 °C for BW and BL. This phenomenon can be attributed to the increase in carbon content and decrease in oxygen content within the hydrochar as the temperature was elevated from 300 to 350 °C. However, in the case of SL, the heating value obtained at 300 °C was almost the same as that at 350 °C. The O/C and H/C ratios of hydrochars were lower than those of their corresponding raw materials. It can be concluded that both dehydration and decarboxylation reactions occurred in the hydrochars after HTL processing. Figure 2 shows a Van Krevelen diagram for the raw materials and hydrochars. Furthermore, opaque regions are included in Fig. 2 to illustrate the diversity of hydrochars, pyrochars, and chars produced from the TCR$^{®}$ process (Hornung et al. 2024). The O/C and H/C ratios of most hydrochars, except for those derived from BL at 300 °C, fell within the lignite and coal regions. These values place them between the ratios typically observed for pyrochar from pyrolysis and hydrochar produced through HTC (Hornung et al. 2024). The decrease of the O/C ratio starting from the dry matter of BL is significant. Hydrochars produced from

Table 2 Mass yields and properties of hydrochars produced from HTL of Beech wood, lignin, and black liquor

	HTL Conditions			Proximate analysis, wt%			Elemental analysis, wt%											
Sample	T, °C	Time, min	SF[a]	VM[b]	FC[c]	A[d]	C	H	N	S	O[e]	O/C[f]	H/C[f]	Mass Yields (wt%)	HHV[g], MJ kg^{-1}	EDR[h]	EY[i], %	FR[j]
BW	300	20	7.19	50.05	48.64	1.31	71.86	5.09	0.27	-	22.78	0.24	0.85	31.11	27.49	1.83	56.98	0.97
BW	350	20	10.22	44.42	53.95	1.63	76.42	4.97	0.31	-	18.30	0.18	0.78	25.92	29.66	1.98	51.22	1.21
SL	300	20	7.19	51.28	48.67	0.05	74.41	5.92	0.65	0.25	18.77	0.19	0.95	32.70	30.28	1.32	43.01	0.95
SL	350	20	10.22	45.84	51.03	3.13	76.04	5.83	0.74	0.16	17.23	0.17	0.92	29.62	30.97	1.35	39.85	1.11
BL	300	20	7.19	45.60	35.50	18.90	53.38	4.20	0.22	1.34	40.86	0.57	0.94	31.37	16.87	0.73	22.85	0.78
BL	350	20	10.22	37.61	52.24	10.15	69.74	5.05	0.27	1.03	23.91	0.26	0.87	27.29	26.61	1.15	31.36	1.39

[a]SF: Severity factor, [b]VM: Volatile matter, [c]FC: Fixed carbon, [d]Ash, [e]by difference, [f]Atomic ratios, [g]HHV: Higher heating value, [h]EDR: Energy densification ratio, [i]EY: Energy yield, [j]FR: Fuel ratio

BL contained alkaline salts, such as hydroxides and carbonates, with traces of these salts still present in the hydrochar produced at both 300 and 350 °C. At 350 °C, the ash content of the hydrochar produced from BL decreased (Table 2). Therefore, the 350 °C data point for BL-derived hydrochar in the Van Krevelen diagram is closer to the other produced hydrochars in the lignite and coal region (Fig. 2). There is a linear correlation between SF values and FR values. As SF values increased, FR values also increased. When the temperature was increased from 300 to 350 °C, EY values for BW and SL decreased due to shifting from solid to gaseous or liquid products.

3.3 Structural characteristic of hydrochars

The 13 C CP/MAS NMR spectra of the hydrochars produced from BW, SL and BL are depicted in Fig. 3. The peak observed between 0 and 80 ppm indicates the presence of sp3 hybridized carbons, suggesting the presence of aliphatic carbons (Baccile et al. 2009; Wu Qiong et al. 2017). The peaks appearing between 110 and 160 ppm signify carbon atoms bonded in sp^2 hybridized carbon structures (C=C bonds) (Wu Qiong et al. 2017). The peak observed in the range of 160–225 ppm typically corresponds to C=O groups, with signals near 175 ppm indicating carboxylic acid moieties, and those between 200 and 220 ppm associated with ketones and aldehydes (Baccile et al. 2009; Wu Qiong et al. 2017). The peaks observed between 110 and 160 ppm appeared as broad shoulders in the hydrochars derived from BL, which is a key indicator of aromatic structures.

Figure 4 demonstrates SEM micrographs of hydrochars produced from BW, SL and BL at 300 and 350 °C. The most interesting aspect is the observed structures in relation to the preparation method. It appears that in BL hydrochars, products either precipitate or adsorb due to the insufficient stirring in the micro autoclaves. As a result, spherical structures adhering to each other were exclusively observed on the surface of hydrochars derived from BL, in contrast to the measurements from the 2 L batch reactor. Spherical structures in hydrochars are known as precipitated droplets from liquid products (Titirici and Antonietti 2010; Gong et al. 2023). Porous structures were observed on the surface of hydrochars for all samples at 300 °C and 350 °C; however, they were more evident in samples obtained at 350 °C.

3.4 Thermal stability of hydrochars

Figure 5 illustrates the TG/DTG profiles of hydrochars derived from BW, SL, and BL at temperatures of 300 °C and 350 °C. Differential decomposition behaviors were observed in hydrochars originating from BL, as compared to those from BW and SL. Previous studies have reported

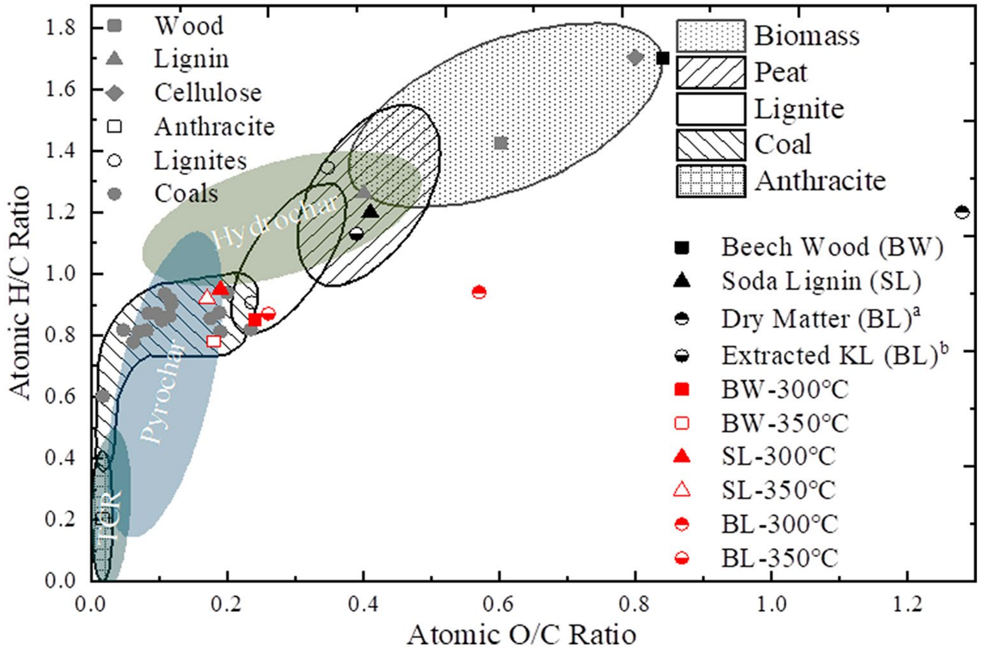

Fig. 2 Van Krevelen Diagram of raw materials and hydrochars

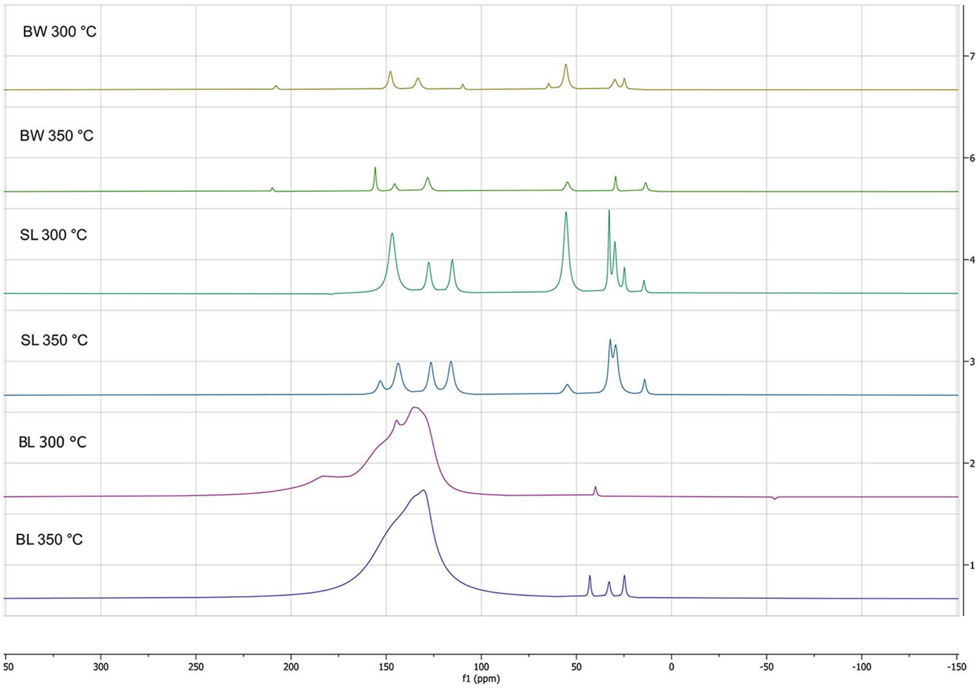

Fig. 3 CP/MAS ^{13}C NMR spectra of hydrochars produced from HTL of BW, SL, and BL at 300 and 350 °C

that the thermal stability of hydrochars depends on both the temperature at which they were obtained and the type of feedstock used (Bach et al. 2015; Nakason et al. 2018; Samadamaeng et al. 2023). However, it should be noted that the temperature at which the hydrochar was obtained plays a more significant role than the type of feedstock used in its production. For hydrochars derived from BL at 300 °C, the initial mass loss was registered between 25 °C and 150 °C, resulting in total weight losses of 10.6 wt% and 4.1 wt% observed during HTL runs conducted at 300 °C and 350 °C, respectively. The decomposition process of BL-derived hydrochars produced at 300 °C occurred in five stages: Stage I (50–150 °C), Stage II (150–350 °C), Stage III (350–500 °C), Stage IV (500–750 °C), and Stage V (825–875 °C). Conversely, hydrochars from BL produced at 350 °C exhibited a four-stage decomposition process: Stage I (25–125 °C), Stage II (150–350 °C), Stage IV (350–600 °C). Relative to BL-derived hydrochars, those from BW and SL exhibited smaller mass losses at temperatures between 25 °C and 150 °C, primarily attributed

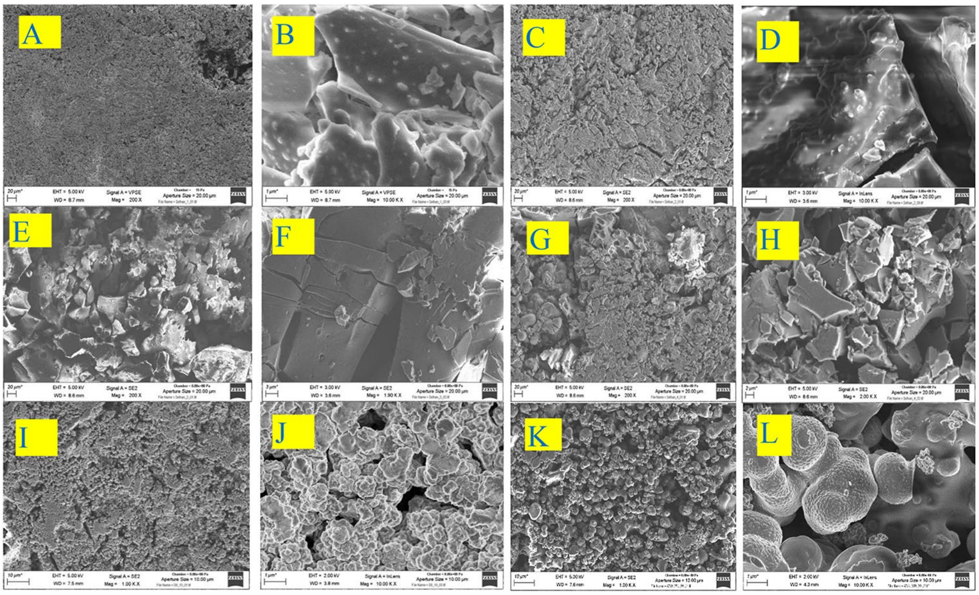

Fig. 4 SEM images of hydrochars produced from HTL of BW, SL, and BL at different magnifications First row: **A**-**B**) BW 300 °C, **C**-**D**) BW 350 °C Second row: **E**-**F**) SL 300 °C, **G**-**H**) SL 350 °C Third row: **I**-**J**) BL 300 °C, **K**-**L**) BL 350 °C

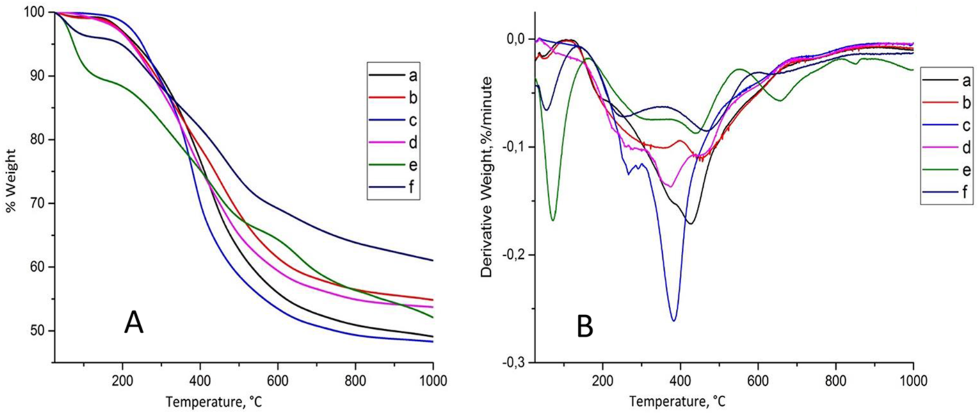

Fig. 5 **A**) TG **B**) DTG of hydrochars produced from HTL of BW, SL, and BL at 300 and 350 °C. [a) BW 300 °C b) BW 350 °C c) SL 300 °C d) SL 350 °C e) BL 300 °C f) BL 350 °C]

to physically adsorbed water. The recorded mass losses in this temperature range (25–150 °C) were as follows: 0.95 wt% for BW-derived hydrochars produced at 300 °C, 1.18 wt% for BW-derived hydrochars produced at 350 °C, 0.37 wt% for SL-derived hydrochars produced at 300 °C, and 1.49 wt% for SL-derived hydrochars produced at 350 °C. The decomposition of hydrochars derived from BW at HTL temperatures of 300 °C and 350 °C occurred in three stages each. At 300 °C, these stages were characterized by: Stage I (25–150 °C), Stage II (150–250 °C), and Stage III (250–650 °C). Similarly, at 350 °C, the decomposition process unfolded through Stage I (0–150 °C), Stage II (150–400 °C), and Stage III (400–650 °C). The decomposition of hydrochars derived from SL at HTL temperatures of 300 °C and 350 °C occurred in two main stages: Stage I (150–300 °C) and Stage II (300–600 °C). Regardless of the type of raw material, hydrochars obtained at 350 °C exhibit higher thermal stability compared to those obtained at 300 °C. Previous research shows that the thermal stability of hydrochars increases with higher production temperatures (Nakason et al. 2018; He et al. 2022; Lin et al. 2024).

3.5 Content of aqueous phases

In this study, the organic phases extracted with ethyl acetate from aqueous phases obtained from HTL of BW, SL, and BL were analyzed using GC-MS/FID, and the results are presented in Table 3. The major compounds detected in BL-derived aqueous phases were phenol, catechol, 3- and 4-methyl catechol, and 4-ethylcatechol. BW and SL derived aqueous phases contained a diverse array of oxygenated compounds, including 2-methylcyclopentanone, phenol, o-cresol, guaiacol, 4-methyl guaiacol, 4-ethylguaiacol, syringol, 4-ethylphenol, catechol, and vanillin. Guaiacol and its derivatives were not observed in the aqueous phases from HTL of BL, likely due to their conversion into catechol and its alkylated compounds. The formation of phenolic compounds from HTL of lignin, beech wood, and black liquor has also been reported by others (Wahyudiono et al.

Table 3 Identified compounds in aqueous phase from beech wood, soda lignin and black liquor at 300 and 350 °C for 20 min

Name of compounds	BW-300 °C (mg/L)	BW-350 °C (mg/L)	SL-300 °C (mg/L)	SL-350 °C (mg/L)	BL-300 °C (mg/L)	BL-350 °C (mg/L)
2-Methylcyclopentanone	5.8	19.4	10.0	24.1	-	-
Phenol	30.9	44.6	243.7	530.7	33.7	24.7
o-Kresol	9.4	15.9	8.4	40.4	-	-
Guaiacol	141.1	166.1	1011.4	567.5	-	-
4-Ethylphenol	4.0	4.0	92.1	179.5	-	-
Catechol	133.9	288.4	423.2	2741.5	1400.7	246.9
4-Methylguaiacol	19.1	43.7	162.9	133.2	-	-
4-Ethylguaiacol	14.0	16.8	175.0	130.6	-	-
Syringol	397.5	270.8	774.0	-	-	-
4-Ethylcatechol	7.5	33.2	60.6	638.0	-	-
4-Methylcatechol	30.3	92.3	62.2	1025.2	-	-
Vanillin	38.8	39.1	13.7	8.7	-	-
3-Methoxycatechol	145.1	499.8	639.8	-	-	-
3-Methylcatechol	20.2	-	-	767.3	99.5	222.8
4-Methylcatechol	-	-	-	-	1011.4	524.2
4-Ethylcatechol					255.6	209.9
3,4 Dihydroxyacetophenone	27.5	24.6	10.8	68.4	-	-
Syringaldehyde	28.2	33.7	36.6	65.9	-	-
Acetosyringone	-	4.4	6.6	6.1	-	-

2007; Kang et al. 2011; Tekin et al. 2013; Orebom et al. 2018; Demirkaya et al. 2024). Low molecular weight phenolic compounds such as guaiacol and catechol are known to contribute to the formation of hydrochar in the cases of SL and BL (Kang et al. 2013). In the case of BW, in addition to these phenolic compounds, furan derivatives deriving from cellulose (which we were unable to quantify under our analytical method conditions) and compounds derived from furans such as 2-methyl-cyclopenten-1-one and its derivatives (detected by GC-MS) are responsible for the formation of hydrochars.

4 Conclusion

This study highlighted the influence of biomass type and temperature on the yields and properties of hydrochars from beech wood (BW), soda lignin (SL), and black liquor (BL) via hydrothermal liquefaction (HTL) at 300 °C and 350 °C for 20 min. BW derived hydrochars had the highest carbon yields, while SL derived hydrochars showed the highest mass yields. Increased temperature enhanced the fuel ratio, improving energy potential. BL derived hydrochars had the highest ash content, while SL hydrochars exhibited the best heating values. Solid-state NMR and SEM analyses revealed distinct structural characteristics, and thermal analysis indicated that hydrochars produced at 350 °C had better thermal stability. The study suggests that hydrochars have high potential for applications in carbon sequestration and solid biofuel production, with properties that can be tailored by adjusting processing conditions.

Supplementary Information The online version contains supplementary material available at https://doi.org/10.1007/s00107-025-02214-2 .

Acknowledgements We express our sincere gratitude to Mr. Thomas Tietz, Mr. Armin Lautenbach, Mrs. Birgit Rolli, and Mr. Yannick Träutlein for their invaluable technical supports.

Author contributions Maximilian Wörner: Data curation, Investigation, Methodology, Writing-original draft. Ursel Hornung: Data curation, Investigation, Methodology, Writing-review & editing, Supervision. Selhan Karagoz: Investigation, Methodology, Conceptualization, Writing-original draft. Thomas Zevaco: Data curation, Investigation, Methodology. Nicolaus Dahmen: Conceptualization, Writing-review & editing.

Funding Open Access funding enabled and organized by Projekt DEAL.

Data availability No datasets were generated or analysed during the current study.

Declarations

Competing interests The authors declare no competing interests.

References

Alper K, Tekin K, Karagöz S (2019) Hydrothermal Liquefaction of Lignocellulosic Biomass using Potassium Fluoride-Doped Alumina. Energy Fuels 33:3248–3256. https://doi.org/10.1021/acs.energyfuels.8b04381

Aykaç GN, Tekin K, Akalın MK et al (2018) Production of crude bio-oil and biochar from hydrothermal conversion of jujube stones with metal carbonates. Biofuels 9:613–623. https://doi.org/10.1080/17597269.2018.1442661

Baccile N, Laurent G, Babonneau F et al (2009) Structural characterization of hydrothermal carbon spheres by advanced solid-state MAS 13 C NMR investigations. J Phys Chem C 113:9644–9654

Bach Q-V, Tran K-Q, Skreiberg Ø, Trinh TT (2015) Effects of wet torrefaction on pyrolysis of woody biomass fuels. Energy 88:443–456

Cao Y, Zhang C, Tsang DCW et al (2020) Hydrothermal liquefaction of lignin to aromatic chemicals: impact of Lignin structure. Ind Eng Chem Res 59:16957–16969. https://doi.org/10.1021/acs.iecr.0c01617

Cheng S, D'cruz I, Wang M et al (2010) Highly efficient liquefaction of Woody Biomass in Hot-compressed alcohol – water co-solvents. Energy Fuels 24:4659–4667. https://doi.org/10.1021/ef901218w

Dahdouh A, Le Brech Y, Khay I et al (2023) Hydrothermal liquefaction of Moroccan two-phase olive mill waste (alperujo): Parametric study and products characterizations. Ind Crops Prod 205:117519

De Caprariis B, De Filippis P, Petrullo A, Scarsella M (2017) Hydrothermal liquefaction of biomass: influence of temperature and biomass composition on the bio-oil production. Fuel 208:618–625

Demirbaş A (2001) Relationships between lignin contents and heating values of biomass. Energy Conv Manag 42:183–188

Demirkaya E, Cocero MJ, Cantero D (2024) Supercritical water depolymerization of black liquor, refining and comprehensive analysis of products including biopolyols. J Supercrit Fluids 211:106296

Elliott DC, Biller P, Ross AB et al (2015) Hydrothermal liquefaction of biomass: developments from batch to continuous process. Bioresour Technol 178:147–156

Gong Y, Xie L, Chen C et al (2023) Bottom-up hydrothermal carbonization for the precise engineering of carbon materials. Prog Mater Sci 132:101048

Haarlemmer G, Guizani C, Anouti S et al (2016) Analysis and comparison of bio-oils obtained by hydrothermal liquefaction and fast pyrolysis of beech wood. Fuel 174:180–188

Harisankar S, Vinu R (2023) Platform chemicals from hardwood black liquor via hydrothermal liquefaction: influence of process conditions on product yields and quality. Sustainable Energy Fuels 7:4423–4441

He Q, Cheng C, Raheem A et al (2022) Effect of hydrothermal carbonization on woody biomass: from structure to reactivity. Fuel 330:125586

Hornung A, Stenzel F, Grunwald J (2024) Biochar—just a black matter is not enough. Biomass Conv Bioref 14:5889–5900. https://doi.org/10.1007/s13399-021-01284-5

Hu J, Shen D, Wu S et al (2014) Effect of temperature on structure evolution in char from hydrothermal degradation of lignin. J Anal Appl Pyrol 106:118–124

Isikgor FH, Becer CR (2015) Lignocellulosic biomass: a sustainable platform for the production of bio-based chemicals and polymers. Polym Chem 6:4497–4559

Jayathilake M, Rudra S, Akhtar N, Christy AA (2021) Characterization and evaluation of hydrothermal liquefaction char from alkali lignin in subcritical temperatures. Materials 14:3024

Kang S, Li X, Fan J, Chang J (2011) Classified separation of Lignin Hydrothermal Liquefied products. Ind Eng Chem Res 50:11288–11296. https://doi.org/10.1021/ie2011356

Kang S, Li X, Fan J, Chang J (2013) Hydrothermal conversion of lignin: a review. Renew Sustain Energy Rev 27:546–558

Lin H, Li C, Jiang Y et al (2024) Hydrothermal carbonization of pretreated pine needles: the impacts of temperature and atmosphere in pretreatment on structural evolution of hydrochar. J Anal Appl Pyrol 106421

Ma Q, Han L, Huang G (2018) Effect of water-washing of wheat straw and hydrothermal temperature on its hydrochar evolution and combustion properties. Bioresour Technol 269:96–103

Madsen RB, Bernberg RZ, Biller P et al (2017) Hydrothermal co-liquefaction of biomasses–quantitative analysis of bio-crude and aqueous phase composition. Sustainable Energy Fuels 1:789–805

Musa U, Castro-Díaz M, Uguna CN, Snape CE (2022) Effect of process variables on producing biocoals by hydrothermal carbonisation of pine Kraft lignin at low temperatures. Fuel 325:124784

Nakason K, Panyapinyopol B, Kanokkantapong V et al (2018) Hydrothermal carbonization of unwanted biomass materials: Effect of process temperature and retention time on hydrochar and liquid fraction. J Energy Inst 91:786–796

Nan W, Shende AR, Shannon J, Shende RV (2016) Insight into Catalytic Hydrothermal Liquefaction of Cardboard for Biofuels Production. Energy Fuels 30:4933–4944. https://doi.org/10.1021/acs.energyfuels.6b00479

Orebom A, Verendel JJ, Samec JSM (2018) High yields of Bio oils from Hydrothermal Processing of Thin Black Liquor without the Use of catalysts or Capping agents. ACS Omega 3:6757–6763. https://doi.org/10.1021/acsomega.8b00854

Ragauskas AJ, Williams CK, Davison BH et al (2006) The path forward for biofuels and biomaterials. Science 311:484–489

Rivas-Arrieta MJ, Torri C, Rombolà AG, Biller P (2024) Hydrochar fractionation and composition in batch and continuous hydrothermal liquefaction. Biomass Bioenergy 183:107166

Samadamaeng N, Suttinun O, Sawatdeenarunat C, Charnnok B (2023) Enhanced integrative process of hydrothermal carbonization and anaerobic digestion with hydrochar addition from lignocellulosic waste. Biomass Convers Biorefinery 1–11

Soh L, Eckelman MJ (2016) Green Solvents in Biomass Processing. ACS Sustainable Chem Eng 4:5821–5837. https://doi.org/10.1021/acssuschemeng.6b01635

Tai L, De Caprariis B, Scarsella M et al (2021) Improved Quality Bio-crude from Hydrothermal Liquefaction of Oak Wood assisted by zero-Valent metals. Energy Fuels 35:10023–10034. https://doi.org/10.1021/acs.energyfuels.1c00889

Tekin K, Akalın MK, Bektaş S, Karagöz S (2013) Hydrothermal wood processing using borax decahydrate and sodium borohydride. J Anal Appl Pyrol 104:68–72

Tekin K, Karagöz S, Bektaş S (2014) A review of hydrothermal biomass processing. Renew Sustain Energy Rev 40:673–687

Titirici M-M, Antonietti M (2010) Chemistry and materials options of sustainable carbon materials made by hydrothermal carbonization. Chem Soc Rev 39:103–116

Toor SS, Rosendahl L, Rudolf A (2011) Hydrothermal liquefaction of biomass: a review of subcritical water technologies. Energy 36:2328–2342

Vadlamudi DP, Pecchi M, Sudibyo H, Tester JW (2024) Direct and two-stage Hydrothermal Liquefaction of Chicken Manure: impact of reaction parameters on Biocrude Oil Upgradation. ACS Sustainable Chem Eng 12:4300–4313. https://doi.org/10.1021/acssuschemeng.3c08579

Vassilev SV, Baxter D, Andersen LK et al (2012) An overview of the organic and inorganic phase composition of biomass. Fuel 94:1–33

Wahyudiono, Kanetake T, Sasaki M, Goto M (2007) Decomposition of a Lignin Model Compound under Hydrothermal Conditions. Chem Eng & Technol 30:1113–1122. https://doi.org/10.1002/ceat.200700066

Wörner M, Barsuhn A, Zevaco T et al (2024) From pulp to aromatic ProductsReaction pathways of Lignin Depolymerization. Energy Fuels 38:6020–6035. https://doi.org/10.1021/acs.energyfuels.3c04509

Wu Q, Huang L, Yu S, Liu S, Xie C, Ragauskas AJ (2017) Structural elucidation of hydro-products from hydrothermal carbonization of loblolly pine at different temperatures using NMR techniques. Energy 133:171–8

Zanon Costa C, Falabella Sousa-Aguiar E, Peixoto Gimenes Couto MA, Souza de Carvalho Filho JF (2020) Hydrothermal treatment of vegetable oils and fats aiming at yielding hydrocarbons: a review. Catalysts 10:843

Zhan Y, Cheng J, Liu X et al (2022) Assessing the availability of two bamboo species for fermentable sugars by alkaline hydrogen peroxide pretreatment. Bioresour Technol 349:126854

Zhong C, Wei X (2004) A comparative experimental study on the liquefaction of wood. Energy 29:1731–1741